

Density Functional Theory Prediction of the Relative Energies and Isotope Effects for the Concerted and Stepwise Mechanisms of the Diels–Alder Reaction of Butadiene and Ethylene

E. Goldstein,^{*,†} Brett Beno,[‡] and K. N. Houk^{*,‡}

Contribution from the Department of Chemistry and Biochemistry, University of California, Los Angeles, Los Angeles, California 90095-1569, and Department of Chemistry, California State Polytechnic University, Pomona, 3801 West Temple Avenue, Pomona, California 91768

Received January 17, 1996. Revised Manuscript Received April 8, 1996[⊗]

Abstract: Density-functional theory has been applied to the study of the mechanism of the Diels–Alder reaction of butadiene and ethylene. Both synchronous concerted and two-step diradical mechanisms were studied at the Becke3LYP/6-31G* level. The lowest energy stepwise pathway has a free energy of activation 7.7 kcal/mol above that of the concerted path. Spin correction of the spin-contaminated diradical transition structure energy reduces this energy difference to 2.3 kcal/mol. A study of the H₂ potential energy surface suggests that the spin-projection procedure overcorrects the energies of diradical species; the diradical energies likely fall between the corrected and uncorrected values. Thus, the free energy of concert for the Diels–Alder reaction is predicted to be between 2.3 and 7.7 kcal/mol, in excellent agreement with thermochemical estimates. Energies of reaction and geometries of the reactants and product are in good agreement with available experimental results. Calculated secondary kinetic isotope effects agree well with experimental data on a related reaction, and support a concerted mechanism for the butadiene plus ethylene Diels–Alder reaction. The Becke3LYP DFT method is capable of relatively economical direct comparisons of concerted and stepwise mechanisms.

Introduction

The Diels–Alder reaction mechanism has been the subject of controversy which has only recently led to consensus.^{1a} The parent reaction of butadiene and ethylene is concerted, but the activation barrier for the stepwise mechanism is only a few kcal/mol higher.¹ It is difficult to reproduce this difference computationally, since both dynamical and non-dynamical correlation energy corrections must be included in order to obtain accurate relative energies of closed-shell and open-shell (diradical) species.^{1c} This is a general problem in the study of pericyclic reactions, which may occur via either concerted (closed-shell) or stepwise (open-shell) mechanisms.

Recently, density-functional theory (DFT)² with nonlocal gradient corrections has been shown to be an economical way to calculate bond dissociation energies;³ accurate results require a balanced treatment of even- and odd-electron species. The successful calculation of singlet–triplet gaps in carbenes and related species indicates that DFT can also reproduce energy

differences between closed-shell and open-shell species.⁴ These features suggest that DFT might prove useful for the direct comparison of concerted and stepwise mechanisms of Diels–Alder and other pericyclic reactions. In this study, the potential surfaces for the concerted and stepwise pathways of the Diels–Alder reaction of butadiene and ethylene are examined with DFT. The previous DFT studies of this reaction have been confined to the concerted regime.⁵ We find that the Becke3LYP functional with the 6-31G* basis set produces excellent geometries and energies for both concerted and stepwise paths. Spin correction is performed on the spin-contaminated systems to provide refined energy estimates. The performance of the spin correction procedure is tested on H₂ dissociation. These results show that DFT can be an effective tool for the simultaneous study of both concerted and stepwise paths of many pericyclic reactions.

Background

We have recently reviewed computational investigations of the reaction of butadiene and ethylene and related Diels–Alder reactions.^{1a–c} Previous theoretical studies of the Diels–Alder reaction have ranged from semiempirical methods to ab initio techniques including Hartree–Fock (HF), Møller–Plesset (MP_n), and multiconfiguration-self-consistent-field (MCSCF) methods. The results of different ab initio studies are in qualitative agreement regarding the geometries and energies of the concerted transition state, while MCSCF and restricted Hartree–Fock (RHF) calculations with limited configuration interaction (CI) give similar results for the stepwise diradical paths.¹ For diradicals, unrestricted Hartree–Fock (UHF) methods, as well

[†] California State Polytechnic University, Pomona.

[‡] University of California, Los Angeles.

[⊗] Abstract published in *Advance ACS Abstracts*, June 1, 1996.

(1) (a) Houk, K. N.; González, J.; Li, Y. *Acc. Chem. Res.* **1995**, *28*, 81. (b) Houk, K. N.; Li, Y.; Evanseck, J. D. *Angew. Chem., Int. Ed. Engl.* **1992**, *31*, 682. (c) Borden, W. T.; Loncharich, R. J.; Houk, K. N. *Ann. Rev. Phys. Chem.* **1988**, *39*, 213. (d) Houk, K. N.; Lin, Y.-T.; Brown, F. K. *J. Am. Chem. Soc.* **1986**, *108*, 554. (e) Li, Y.; Houk, K. N. *J. Am. Chem. Soc.* **1993**, *115*, 7478. (f) Storer, J. W.; Raimondi, L.; Houk, K. N. *J. Am. Chem. Soc.* **1994**, *116*, 9675. (g) Townshend, R. E.; Ramunni, G.; Segal, G.; Hehre, W. J.; Salem, L. *J. Am. Chem. Soc.* **1976**, *98*, 2190. (h) Dewar, M. J. S.; Olivella, S.; Stewart, J. J. P. *J. Am. Chem. Soc.* **1986**, *108*, 5771.

(2) (a) Kohn, W.; Sham, L. J. *Phys. Rev.* **1965**, *140*, A1133. (b) Hohenberg, P.; Kohn, W. *Phys. Rev.* **1964**, *136*, B864. For reviews see: (c) Ziegler, T. *Chem. Rev.* **1991**, *91*, 651. (d) *Density Functional Methods in Chemistry*; Labanowski, J., Andzelm, J., Eds.; Springer: Berlin, 1991. (e) Parr, R. G.; Yang, W. *Density-Functional Theory of Atoms and Molecules*; Oxford University Press: New York, 1989.

(3) Johnson, B. G.; Gill, P. M. W.; Pople, J. A. *J. Chem. Phys.* **1993**, *98*, 5612.

(4) Cramer, C. J.; Dulles, F. J.; Storer, J. W.; Worthington, S. E. *Chem. Phys. Lett.* **1994**, *218*, 387.

(5) (a) Stanton, R. V.; Merz, K. M., Jr. *J. Chem. Phys.* **1993**, *100*, 434. (b) Carpenter, J. E.; Sosa, C. P. *J. Mol. Struct. (Theochem)* **1994**, *311*, 325. (c) Jurisic, B.; Zdravkovski, Z. *J. Chem. Soc., Perkin Trans. 2* **1995**, 1223.

as dynamical correlation energy corrections, are necessary to provide even qualitatively reasonable results.⁶ RHF methods favor closed-shell or synchronous mechanisms, while UHF and semiempirical treatments are biased toward diradical pathways. Computationally intensive methods such as multireference configuration interaction (MRCI)^{7a} or complete active space perturbation theory (CASPT2)^{7b,c} are necessary to provide a balanced treatment of concerted (closed-shell) and diradical (open-shell) mechanisms. The long-standing mechanistic controversy has now led to agreement^{1a,c} that the concerted transition state is more stable than the first transition state for the stepwise process by 2–7 kcal/mol.⁸ Comparisons of theoretical and experimental secondary kinetic isotope effects confirm that the concerted pathway is favored.^{1f,9}

The computational requirements for CASSCF and other post-HF computations are extremely demanding.^{1e,10,11} For the Diels–Alder biradical and concerted potential surfaces, which include numerous possible reaction pathways, it is especially costly to include all configurations for all the resulting stationary points.

DFT offers improvements both in computational efficiency^{3,4,12} and in a balanced treatment of open- and closed-shell systems.^{2c,12bc,13} Initial NL-DFT results for hydrogenations, isodesmic reactions, bond dissociations, and proton affinities are encouraging.^{3,12ade,14} Overall, the nonlocal spin density (NLS) method provides energetics superior to HF results and comparable to those of MP2/HF methods.^{3,5,12,14a,15} Unlike enthalpies of reactions, the structures of transition states and shapes of potential energy surfaces are difficult or impossible to investigate experimentally. Until recently, post-HF calculations have been the most reliable source of information.^{5,12a,14,16}

NLS DFT studies on the concerted Diels–Alder transition state give results closely matching those from post-HF calculations.⁵ Carpenter and Sosa, Jursic and Zdravkovski, and Stanton

and Merz have independently examined the differences between local and nonlocal DFT on the concerted transition state energies and geometries, using a variety of basis sets.⁵ Jursic and co-workers^{5c} also focused on the HF-DFT hybrid methods which are particularly effective. The BLYP^{3,12e,15a,b} and Becke3LYP^{12a} hybrid density-functional method using the 6-31G** basis set yield accurate values for the barrier height of the concerted pathway.^{5c} Stanton^{5a} has shown that the local density-functional (LDF) approach yields an extremely low barrier height, while Carpenter^{5b} has shown that the NLS method gives better agreement with the experimental value. The NLS method also predicts an energy of reaction in excellent agreement with the experimental value.^{5b}

We have investigated the use of hybrid HF-DFT for direct comparison of closed-shell and diradical surfaces involved in the concerted and stepwise Diels–Alder mechanisms. In this paper, we compare calculated energies to experimental data and geometries to previous CASSCF calculations. We also calculate the secondary kinetic isotope effects (SKIE)¹⁷ and compare these to experiment and to previous calculations.^{18,19} This provides an alternative way to assess whether the calculated geometries and vibrational frequencies are reasonable.

The Diels–Alder Mechanism. The Diels–Alder reaction of butadiene and ethylene²⁰ is exothermic by 40 kcal/mol and has a reaction barrier of 27.5 kcal/mol.²¹ It may occur by synchronous or asynchronous concerted mechanisms, or by a nonconcerted stepwise mechanism (Figure 1). Thermochemical estimates indicate that the activation energies for formation of possible diradical intermediates are only slightly higher than the experimental barrier.⁸ The lowest energy diradical should be formed via *s-trans*-butadiene. Because the barrier for rotation about the allylic C–C bond in the diradical intermediate (~14 kcal/mol) is greater than that expected for reversion of the diradical to butadiene and ethylene, this will not be a likely route to cyclohexene. However, it may be important in related reactions, such as vinylcyclobutane formation or radical copolymerizations.²²

There are three conceivable diradicals formed from *s-cis*-butadiene. These are labeled as anti, gauche-in, and gauche-out in Figure 1. To cyclize, all must pass through a geometry like the gauche-in diradical, with the radical centers near each other. Among the many previous calculations, the pioneering work by Salem and co-workers^{1g} is of special note, since it included CI and exploration of the whole potential surface, even

(6) (a) Chipman, D. M. *Theor. Chim. Acta* **1992**, *82*, 93 and references therein. (b) Sekino, H.; Bartlett, R. J. *J. Chem. Phys.* **1985**, *82*, 4225.

(7) (a) Roos, B. O. In *Ab Initio Methods in Quantum Chemistry II*; Lawley, K. P., Ed.; Wiley: New York, 1987; p 399. (b) Andersson, K.; Malmqvist, P.-Å.; Roos, B. O.; Sadlej, A. J.; Wolinski, K. *J. Phys. Chem.* **1990**, *94*, 5483. (c) Andersson, K.; Malmqvist, P. A.; Roos, B. O. *J. Chem. Phys.* **1992**, *96*, 1218.

(8) Doering, W. v. E.; Roth, W. R.; Breuckmann, R.; Figge, L.; Lennartz, H.-W.; Fessner, W.-D.; Prinzbach, H. *Chem. Ber.* **1988**, *121*, 1.

(9) Houk, K. N.; Li, Y.; Storer, J.; Raimondi, L.; Beno, B. *J. Chem. Soc., Faraday Trans.* **1994**, *90*, 1599.

(10) Bernardi, F.; Bottoni, A.; Field, M. J.; Guest, M. F.; Hillier, I. H.; Robb, M. A.; Venturini, A. *J. Am. Chem. Soc.* **1988**, *110*, 3050.

(11) (a) MCSCF: Fernandez, B.; Jørgensen, P.; Simons, J. *J. Chem. Phys.* **1993**, *98*, 7012. (b) Coupled cluster methods: Carmichael, I. *J. Chem. Phys.* **1989**, *91*, 1072 and references therein. (c) MRCI: Feller, D.; Glendening, E. D.; McCullough, E. A., Jr.; Miller, R. J. *J. Chem. Phys.* **1993**, *99*, 2829.

(12) (a) Smith, B. J.; Radom, L. *Chem. Phys. Lett.* **1994**, *231*, 345. (b) Johnson, B. G.; Gonzalez, C. A.; Gill, P. M. W.; Pople, J. A. *Chem. Phys. Lett.* **1994**, *221*, 100. (c) Barone, V.; Adamo, C.; Russo, N. *Chem. Phys. Lett.* **1993**, *212*, 5. (d) Andzelm, J.; Wimmer, E. *J. Chem. Phys.* **1992**, *96*, 1280. (e) Gill, P. M. W.; Johnson, B. G.; Pople, J. A.; Frisch, M. J. *Chem. Phys. Lett.* **1992**, *197*, 499.

(13) (a) Eriksson, L. A.; Malkina, O. L.; Malkin, V. G.; Salahub, D. R. *J. Chem. Phys.* **1994**, *100*, 5066. (b) Eriksson, L. A.; Malkin, V. G.; Malkina, O. L.; Salahub, D. R. *J. Chem. Phys.* **1993**, *99*, 9756. (c) Ishii, N.; Shimizu, T. *Phys. Rev. A* **1993**, *48*, 1691. (d) Akai, H.; Akai, M.; Blugel, S.; Dritter, B.; Ebert, H.; Terakura, K.; Zeller, R.; Dedericks, P. H. *Prog. Theor. Phys. Suppl.* **1990**, *101*, 11.

(14) See refs 2c–e, 3 and: (a) Andzelm, J.; Sosa, C.; Eades, R. A. *J. Phys. Chem.* **1993**, *97*, 4664. (b) Fan, L.; Ziegler, T. *J. Chem. Phys.* **1990**, *92*, 3645.

(15) (a) Murray, C. W.; Laming, G. J.; Handy, N. C.; Amos, R. D. *Chem. Phys. Lett.* **1992**, *199*, 551. (b) Gill, P. M. W.; Johnson, B. G.; Pople, J. A.; Frisch, M. J. *Int. J. Quantum Chem. Symp.* **1992**, *26*, 319. (c) Murray, C. W.; Handy, N. C.; Amos, R. D. *J. Chem. Phys.* **1993**, *98*, 7145.

(16) Grodzicki, M.; Seminario, J. M.; Politzer, P. *J. Chem. Phys.* **1991**, *94*, 1668.

(17) For review and general kinetic isotope articles see: (a) Carpenter, B. *Determination of Organic Reaction Mechanisms*; Wiley-Interscience: New York, 1986; pp 83–111. (b) Melander, L.; Saunders, W. H., Jr. *Reaction Rates of Isotopic Molecules*; Wiley: New York, 1980. (c) Gajewski, J. J. In *Isotope Effects in Organic Chemistry: Secondary and Solvent Isotope Effects*; Buncl, E., Lee, C. C., Eds.; Elsevier: New York, 1987; Vol. 7, pp 115–176. (d) Streitwieser, A., Jr.; Jagow, R. H.; Fahey, R. C.; Suzuki, S. *J. Am. Chem. Soc.* **1958**, *80*, 2326. (e) Saunders, W. H., Jr. In *Techniques of Chemistry: Investigations of Rates and Mechanisms of Reactions*; Bernasconi, C. F., Ed.; Wiley-Interscience: New York, 1980; Vol. 6, pp 565–611.

(18) (a) Singleton, D. A.; Thomas, A. A. *J. Am. Chem. Soc.* **1995**, *117*, 9357. (b) Seltzer, S. *J. Am. Chem. Soc.* **1963**, *85*, 1360. (c) Gajewski, J. J.; Peterson, K. B.; Kagel, J. R.; Huang, Y. C. *J. Am. Chem. Soc.* **1989**, *111*, 9078. (d) Van Sickle, D. E.; Rodin, J. O. *J. Am. Chem. Soc.* **1964**, *86*, 3091. (e) Taagepera, M.; Thornton, E. R. *J. Am. Chem. Soc.* **1972**, *94*, 1168.

(19) See for example, ref 1 and: (a) Houk, K. N.; Gustafson, S. M.; Black, K. A. *J. Am. Chem. Soc.* **1992**, *114*, 8565. (b) Dewar, M. J. S.; Olivella, S.; Rzepa, H. S. *J. Am. Chem. Soc.* **1978**, *100*, 5650.

(20) (a) Diels, O.; Alder, K. *Justus Liebig's Ann. Chem.* **1928**, *460*, 98. (b) Woodward, R. B.; Hoffmann, R. *Angew. Chem., Int. Ed. Engl.* **1969**, *8*, 781.

(21) See ref 1b and references therein.

(22) (a) Mikhael, M. G.; Padias, A. B.; Hall, H. K. *Macromolecules* **1993**, *26*, 5835 and references therein. (b) Li, Y.; Padias, A. B.; Hall, H. K. *J. Org. Chem.* **1993**, *58*, 7049. (c) Frey, H. M.; Pottinger, R. *J. Chem. Soc., Faraday Trans. 1* **1978**, *74*, 1827.

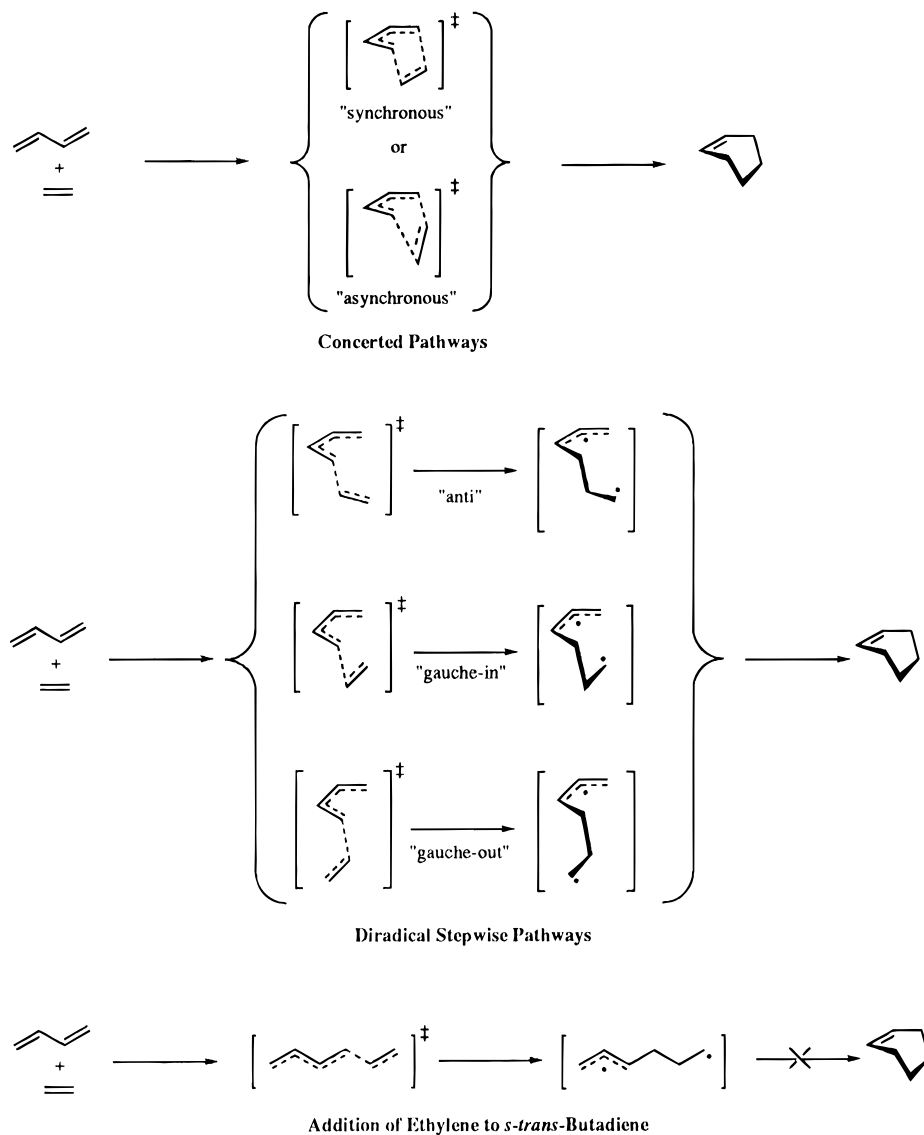


Figure 1. The concerted and stepwise pathways for the Diels–Alder reaction of butadiene with ethylene.

at a very early point in the history of computational chemistry. Salem concluded that the reaction is concerted, proceeding through a C_s symmetrical transition state. A set of distinct diradical pathways and their interconversions were studied with 3×3 CI and the 4-31G basis set. The hex-2-ene-1,6-diyl diradical was found to be an energy minimum. The anti diradical conformer was the most favorable diradical intermediate. The energy of the transition state leading to the anti diradical was 4 kcal/mol above that of the concerted transition state.^{1g} A pathway for the formation of the gauche-in biradical from the concerted TS had a barrier 1.9 kcal/mol above the concerted TS.

Bernardi and co-workers surveyed the full surface of the Diels–Alder reaction using CASSCF/STO-3G calculations.¹⁰ Four transition states for the reaction of ethylene and *s*-cis-butadiene were located. A concerted synchronous pathway with a 35 kcal/mol activation barrier was also located. Three transition states, leading to gauche-in, anti, and gauche-out diradicals, were located. The energies of these transition states were 32–34 kcal/mol above that of the reactants. The gauche-out intermediate closed to vinylcyclobutane with a barrier of 6 kcal/mol. The three intermediates were connected by two transition states which involve rotations about single bonds. Bernardi and co-workers concluded that at the STO-3G level the stepwise diradical path is more favorable than the concerted

mechanism.¹⁰ However, with the larger 4-31G basis set the concerted pathway was favored. Furthermore, with this basis set, the only stationary point located in this region of the surface in addition to the synchronous TS was the gauche-in diradical.

Li and Houk applied the CASSCF/6-31G* method with a 6-electron 6-orbital active space to the concerted C_s synchronous transition state and the stepwise pathway involving the anti diradical.^{1e} Single point energy calculations at the QCISD(T)/6-31G* level based on MCSCF/6-31G* optimized transition structures favored the concerted mechanism by 10 kcal/mol relative to the stepwise mechanism. This difference becomes 6 kcal/mol after corrections using CASSCF/3-21G zero-point energies and entropies. The experimental estimates for this preference range from 2 to 7 kcal/mol.⁸ At the CASSCF/6-31G* + ZPE level, the anti diradical transition structure was found to be 0.5 kcal/mol lower in energy than the concerted transition structure. Entropy correction using CASSCF/3-21G values leads to a 2.4-kcal/mol preference for the diradical pathway. A transition state for cyclization of the gauche-in diradical was located by Storer^{1f} at the UHF/6-31G* level, while efforts to locate a stable gauche-in diradical minimum at the CASSCF/6-31G* level were unsuccessful.^{1e,9}

The geometry of the concerted transition structure remains approximately constant at various semiempirical and ab initio levels.^{1,10,23} RHF methods generally overestimate energies of

Table 1. Experimental and Theoretical Enthalpies of Reaction (kcal/mol) for the Diels–Alder Reaction of Ethylene and Butadiene

method	$-\Delta H_{\text{reaction}}$	ref
experimental	38.4	a
RHF/6-31G*	36.0	1b
MP2/6-31G*	45.9	1b
MP4/6-31G*	49.1	23a
CASSCF/3-21G	12.9	1e
LDF/DZVP	61.5	5b
NLDF/DZVP	37.6	5b
Becke3LYP/6-31G*	36.6	this work, b

^a $\Delta H(800\text{K})$ from: Uchiyama, M.; Tomioka, T.; Amano, A. *J. Phys. Chem.* **1964**, *68*, 1878. ^b Calculated RB/6-31G* total energies (ZPE) in au of ethylene, butadiene, and cyclohexene are -78.58746 (0.05122), -155.99214 (0.08548), and -234.64829 (0.14700), respectively.

activation, while inclusion of limited electron correlation lowers the barrier below the experimental value.^{1e,23a} Energies of activation calculated with MCSCF methods differ more from experiment than the fully correlated QCISD(T) calculations and show the importance of dynamical electron correlation.^{1c}

Computational Methodology

Calculations were performed with GAUSSIAN 94.²⁴ The Becke3LYP hybrid functional was used throughout this work. It consists of the nonlocal exchange functional of Becke's three-parameter set²⁵ and the nonlocal correlation functional of Lee, Yang, and Parr.²⁶ All the functionals are applied to the self-consistent-field HF densities. The 6-31G* basis set was used in all calculations.²⁷

Full geometry optimizations were performed with GAUSSIAN 94 default criteria. For all structures, frequency calculations were performed in order to determine the nature of stationary points, to obtain zero-point vibrational energies (ZPE), and to determine analytical force constants. QUIVER,²⁸ a program based on the Bigeleisen–Meyer equation,²⁹ was used to calculate the SKIEs.

Restricted Becke3LYP/6-31G* (hereafter referred to as RB) was used for closed-shell species: ethylene (**2**), *s-cis*- and *s-trans*-1,3-butadiene (**1**), cyclohexene (**4**), and the concerted transition structure (**3**). For the diradical surface, full optimizations were carried out at the unrestricted Becke3LYP/6-31G* (hereafter referred to as UB) level on the stationary points of the three open-shell pathways: anti, gauche-in, and gauche-out.

The H₂ potential energy surface was studied with UB and CISD³⁰ single-point calculations using the 6-31G* basis set.

Results and Discussion

Reaction Energies. Table 1 summarizes experimental and recent theoretical enthalpies of the butadiene–ethylene reaction including DFT results from this work and other studies. The ZPE corrected RB energy is within 2 kcal/mol of the experi-

(23) (a) Bach, R. D.; McDouall, J. J. W.; Schlegel, H. B.; Wolber, G. J. *J. Org. Chem.* **1989**, *54*, 2931. (b) Bernardi, F.; Bottoni, A.; Robb, M. A.; Field, M. J.; Hillier, I. H.; Guest, M. F. *J. Chem. Soc., Chem. Commun.* **1985**, 1051.

(24) *Gaussian 94* (Revision C.2), Frisch, M. J.; Trucks, G. W.; Schlegel, H. B.; Gill, P. M. W.; Johnson, B. G.; Robb, M. A.; Cheeseman, J. R.; Keith, T. A.; Petersson, G. A.; Montgomery, J. A.; Raghavachari, K.; Al-Latham, M. A.; Zakrzewski, V. G.; Ortiz, J. V.; Foresman, J. B.; Cioslowski, J.; Stefanov, B. B.; Nanayakara, A.; Challacombe, M.; Peng, C. Y.; Ayala, P. Y.; Chen, W.; Wong, M. W.; Andres, J. L.; Replogle, E. S.; Gomperts, R.; Martin, R. L.; Fox, D. J.; Binkley, J. S.; Defrees, D. J.; Baker, J.; Stewart, J. J. P.; Head-Gordon, M.; Gonzalez, C.; Pople, J. A.; Gaussian, Inc.: Pittsburgh, PA, 1995.

(25) Becke, A. D. *J. Chem. Phys.* **1993**, *98*, 5648.

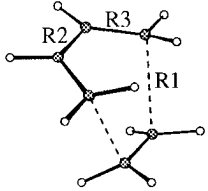
(26) Lee, C.; Yang, W.; Parr, R. G. *Phys. Rev. B* **1988**, *37*, 785.

(27) Hehre, W. J.; Ratom, L.; Schleyer, P. v. R.; Pople, J. A. *Ab Initio Molecular Orbital Theory*; Wiley: New York, 1986.

(28) Saunders, M.; Laidig, K. E.; Wolfsberg, M. *J. Am. Chem. Soc.* **1989**, *111*, 8989.

(29) (a) Bigeleisen, J.; Mayer, M. G. *J. Chem. Phys.* **1947**, *15*, 261. (b) Wolfsberg, M. *Acc. Chem. Res.* **1972**, *5*, 225.

(30) Pople, J. A.; Seeger, R.; Krishnan, R. *Int. J. Quantum Chem. Symp.* **1977**, *11*, 149.

Table 2. Calculated Transition State C–C Bond Lengths and Activation Barriers for the Butadiene plus Ethylene Concerted Diels–Alder Reaction Pathway^a


method	R1	R2	R3	ΔE^\ddagger	ref
experimental				27.5 ± 2	b
RHF/6-31G*	2.201	1.393	1.377	47.4	5b
MP2/6-31G*	2.286	1.410	1.378	20.0	5b
CASSCF/6-31G*	2.223	1.397	1.398	47.4	1e
QCISD(T)/6-31G*// CASSCF/6-31G*	2.223	1.397	1.398	29.1	1e
LDF/DZVP	2.411	1.420	1.368	6.0	5b
NLDF/DZVP	2.322	1.420	1.389	20.4	5b
Becke3LYP/6-31G*	2.273	1.407	1.383	24.8	this work

^a Activation barriers are in kcal/mol and include ZPE; bond lengths are in Å. ^b $E_a(800\text{K})$ from: Rowley, D.; Steiner, H. *Discuss. Faraday Soc.* **1951**, *10*, 198.

mental enthalpy of reaction. Carpenter and co-workers^{5b} showed that while the exothermicity is accurate with the NLDF-DFT approach, it is poor at the LDF level. Table 1 also illustrates the small effect of functional and basis set on the energetics when nonlocal-DFT methods are employed: the hybrid approach, RB, and the nonlocal-DFT method (NLDF/DZVP) agree within 1 kcal/mol. The RB method provides much better results than MP2 or MP4, approaching experimental accuracy at a lower computational cost.

Becke3LYP energies match experimental data better than CASSCF calculations, which predict that the reaction is less exothermic than observed. CASSCF calculations underestimate the exothermicity of the reaction, because the electron correlation in the active space favors π over σ orbitals.^{1c} The hybrid-DFT method handles these orbitals in a more balanced way, by including both non-dynamical and dynamical correlation.^{1c}

Structures and Energetics. Calculated bond lengths are given in Table 2 and Figures 2 and 3. Andzelm and Wimmer found that DFT predicts C–C bond lengths which are too short, and C=C bond lengths which are approximately correct relative to experimental values.^{12d} HF theory frequently gives bond lengths which are too short, while MP2 optimized values are too long.²⁷ The largest deviation from experimental bond lengths for butadiene and ethylene predicted by the RB method is -0.03 Å for the butadiene C₂–C₃ bond. The RB geometry of cyclohexene is in good agreement with experiment.³¹

Table 2 summarizes the concerted transition state geometries and energies calculated at different levels of theory. The RB concerted transition structure (**3**) has forming σ bonds 2.273 Å in length. This value falls between those calculated at the MP2/6-31G* and CASSCF/6-31G* levels, and is shorter than those calculated with other DFT methods. The double bonds of butadiene and ethylene are stretched 25% toward the product geometry, while the C₂–C₃ bond of butadiene is shortened by 40%. RB calculations predict a relatively early transition state for the concerted pathway.

The RB barrier height of 24.8 kcal/mol for the synchronous concerted reaction is within 3 kcal/mol of the measured value (Table 2). CASSCF and RHF methods overestimate, while MP2 underestimates, the activation barrier. The local density-functional approach (LDF/DZVP) underestimates the activation

(31) Chiang, J. F.; Bauer, S. H. *J. Am. Chem. Soc.* **1969**, *91*, 1898.

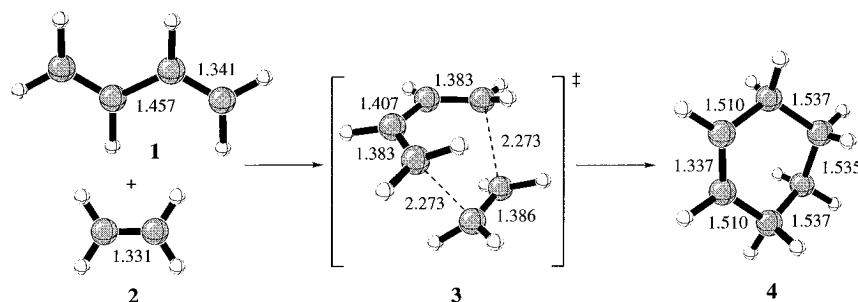


Figure 2. Becke3LYP/6-31G* geometries of reactants (**1** and **2**), concerted transition state (**3**), and product (**4**) of the Diels–Alder reaction of butadiene with ethylene. Bond lengths are in Å.

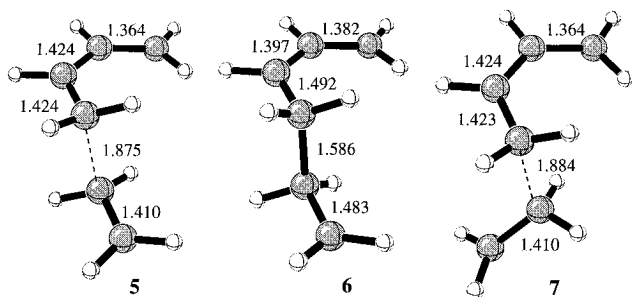


Figure 3. UBcke3LYP/6-31G* geometries of the stepwise anti-diradical transition state (**5**), anti intermediate (**6**), and gauche-out transition state (**7**).

Table 3. Becke3LYP/6-31G* Energies, Entropies, and $\langle S^2 \rangle$ for Stationary Points on the Butadiene plus Ethylene Diels–Alder Potential Energy Surface

molecule	HF energy (au)	ZPE (au)	S (eu)	$\langle S^2 \rangle$
butadiene (1)	−155.99214	0.08548	66.0	0.00
ethylene (2)	−78.58746	0.05122	52.3	0.00
concerted T.S. (3)	−234.54389	0.14056	77.7	0.00
anti T.S. (5)	−234.52695	0.13752	83.5	0.56
intermediate (6)	−234.53466	0.13790	86.1	0.98
gauche-out T.S. (7)	−234.52371	0.13709	84.4	0.61
cyclohexene (4)	−234.64829	0.14700	72.4	0.00

Table 4. Becke3LYP/6-31G* Relative Energies and Entropies of Stationary Points on the Butadiene plus Ethylene Diels–Alder Potential Energy Surface^a

molecule	E_{rel} (kcal/mol)	ΔS_{rel} (eu)
butadiene (1) + ethylene (2)	0.0	0.0
concerted T.S. (3)	24.8	−40.6
anti T.S. (5)	33.6 (28.2)	−34.8
intermediate (6)	29.0 (27.6)	−32.2
gauche-out T.S. (7)	35.3 (29.9)	−33.9
cyclohexene (4)	−36.6	−45.9

^a Relative energies include zero-point corrections. Energies in parentheses are after spin correction.

energy dramatically, while nonlocal DFT with a double- ζ basis set and MP2 calculations give nearly identical results. The QCISD(T)/6-31G**//CASSCF/6-31G* calculation is the only approach thus far which yields results comparable to the hybrid-DFT method.^{1c}

The diradical mechanism was investigated using the UB method. The energies and geometries are summarized in Figure 3 and Tables 3 and 4. The calculations were limited to *s-cis*-butadiene reacting with ethylene in anti (**5** and **6**), gauche-out (**7**), and gauche-in orientations. The search for intermediates was limited to anti and gauche-in structures. The gauche-out intermediate was not investigated here. No evidence for a stable gauche-in diradical was found, in spite of extensive searches. All three intermediates were previously located at the CASSCF/STO-3G level, where the anti intermediate is the most stable,

and the two other diradicals are approximately 1.5 kcal/mol higher in energy.¹⁰ A search for three transition structures resulting from the reaction of *s-cis*-butadiene with ethylene gave the anti (**5**) and gauche-out (**7**) transition structures. The gauche-in could not be located despite repeated attempts. Instead, the concerted transition structure was always obtained. Table 4 shows that transition structure **5** is 4.6 kcal/mol above diradical intermediate **6**. This is reduced to 0.6 kcal/mol after spin projection. Bernardi calculated an 11–12 kcal/mol barrier to reversion to reactants,¹⁰ while Li and Houk found a 5 kcal/mol barrier with CASSCF/6-31G*.^{1c} The diradical nature of transition structure **5** is evident as the C4–C5 forming bond length is 1.88 Å, while the C1–C6 distance is 4.78 Å.

The stepwise mechanism proceeds through intermediate **6**. Attempts to locate the transition state for the closure of **6** to cyclohexene were unsuccessful, leading instead to concerted transition structure **3**. This difficulty was previously reported by Li and Houk in their CASSCF study and indicates that the barrier to closure of the diradical is extremely small.^{1c}

The UB diradical transition structures and intermediates are comparable to those obtained with CASSCF methods.^{1c,10} The UB and CASSCF bond lengths for **5** are within 0.015 Å of each other. The geometry of intermediate **6** matches previous calculations closely.

Unrestricted DFT produces a set of α and β orbitals, in analogy with the UHF method. In DFT theory, these Kohn–Sham orbitals are used to obtain densities, from which energies are evaluated. Pople and co-workers have pointed out that a single determinant of Kohn–Sham orbitals may properly exhibit spin contamination for open-shell systems, since it is the density, not the individual orbitals, which have meaning. The Kohn–Sham determinantal wave function is not a correct wave function for the system, and thus is not an eigenfunction of the S^2 operator.³² In contrast to UHF results,³³ Baker and co-workers³⁴ found that spin contamination is often very small for systems investigated with DFT. Pople and co-workers observed that unrestricted Kohn–Sham (UKS) barriers are lowered by as little as 1 kcal/mol compared to restricted Kohn–Sham (ROKS) barriers. This is further evidence for the low-spin contamination effect.^{12b}

The use of spin-annihilation with DFT calculations has been shown to give improved energies of excited singlet states in butadiene.³⁵ Becke³⁶ has shown that DFT with Noodleman's

(32) Pople, J. A.; Gill, P. M. W.; Handy, N. C. *Int. J. Quantum Chem.* **1995**, 56, 303.

(33) (a) Handy, N. C.; Knowles, P. J.; Somasundram, K. *Theor. Chim. Acta* **1985**, 68, 87. (b) Nobes, R. H.; Pople, J. A.; Radom, L.; Handy, N. C.; Knowles, P. J. *Chem. Phys. Lett.* **1987**, 138, 481.

(34) Baker, J.; Scheiner, A.; Andzelm, J. *Chem. Phys. Lett.* **1993**, 216, 380.

(35) Cramer, C. J.; Dulles, F. J.; Giesen, D. J.; Almlöf, J. *Chem. Phys. Lett.* **1995**, 245, 165.

(36) Edgecombe, K. E.; Becke, A. D. *Chem. Phys. Lett.* **1995**, 244, 427.

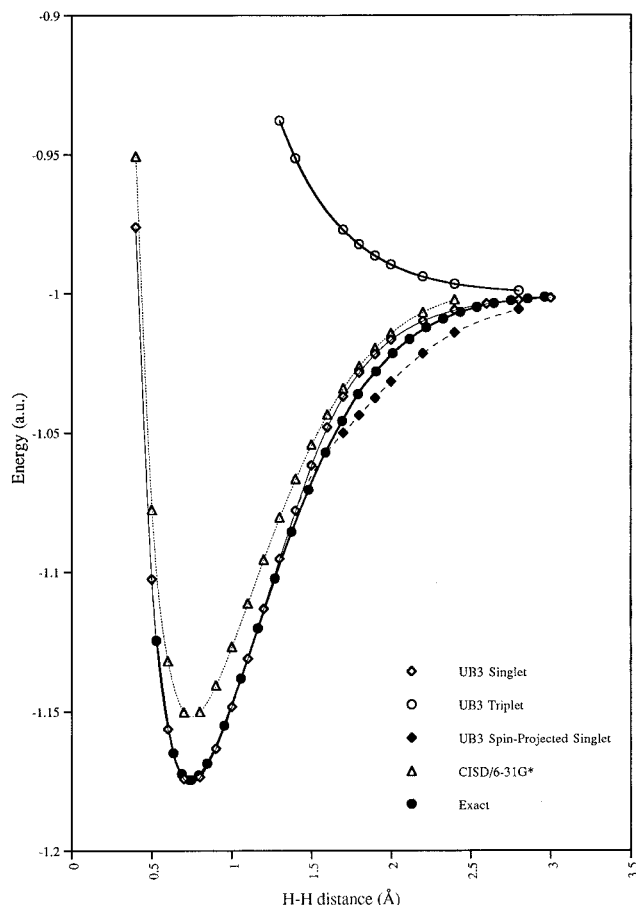


Figure 4. UBecke3LYP/6-31G*, CISD/6-31G*, and exact potential energy surfaces for H₂. Exact singlet surface generated with data from Kolos et al. [Kolos, W.; Wolniewicz, L. *J. Chem. Phys.* **1965**, *43*, 2429; **1968**, *49*, 404].

spin correction³⁷ gives much better results for the bond distance and dissociation energy for the chromium dimer than DFT alone. Yamaguchi and co-workers have also used a similar procedure to obtain improved singlet–triplet energy gaps in monocentric diradicals from UHF, UMP, and UKS calculations.³⁸

Since the Becke3 exchange functional includes some Hartree–Fock exchange, it may be appropriate to perform spin-projection. To evaluate the effect of spin-projection on the singlet energy, we examined the UBecke3LYP/6-31G* singlet, triplet, and spin-corrected singlet surfaces for H₂ dissociation. These are plotted in Figure 4, along with the CISD/6-31G* and exact curves for comparison. Spin-projected energies were calculated with the approximate spin correction procedure proposed by Yamaguchi and co-workers:³⁸

$$\Psi_{(\text{UB})} = c_S {}^1\phi + c_T {}^3\phi$$

$${}^1E_{(\text{SC})} = {}^1E_{(\text{UB})} + f_{\text{SC}}[{}^1E_{(\text{UB})} - {}^3E_{(\text{UB})}]$$

$$f_{\text{SC}} = \frac{c_T^2}{1 - c_S^2} \approx \frac{{}^1\langle S^2 \rangle}{{}^3\langle S^2 \rangle - {}^1\langle S^2 \rangle}$$

Previously, Yamaguchi and co-workers examined the potential energy surfaces for H₂ singlet states using the 6-31G** basis set and B-null, B-LYP, B-PL, and B-P86 methods as well as

with full-CI.^{38b} The DFT surfaces were in good agreement with the full-CI surface, though most methods overestimated and B-null underestimated the stability of the minimum relative to full-CI. Since the DFT methods gave H₂ dissociation curves with qualitatively correct shapes, the effect of spin-projection was not significant.

Figure 4 shows good agreement between the hybrid HF-DFT UB and exact curves in the region of the minimum, while CISD underestimates the stability of H₂. At H–H distances of about 1.3–2.5 Å, the exact and UB singlet curves are divergent, with the DFT curve destabilized relative to the exact curve. The spin-projection procedure outlined above overestimates the stability of the pure singlet states in this region. Thus, the true singlet energy lies between the spin-contaminated and spin-projected singlet energies. Since the spin-projection procedure overcorrects for triplet contamination, the “corrected” energy is not a better approximation of the true singlet energy. However, the spin-contaminated and spin-projected energies provide upper and lower bounds to the true singlet energy. Thus, a range of values can be identified within which the true singlet energy lies.

Table 3 shows that $\langle S^2 \rangle$ values of the reactants (**1** and **2**), product (**4**), and concerted transition structure (**3**) are equal to 0.00. The concerted transition structure (**3**) is not UHF unstable; the RB and UB energies are identical. Initial $\langle S^2 \rangle$ values for the diradical stationary points (**5**–**7**) range from 0.56 to 0.98 and become 0.07 to 0.23 after spin annihilation. These deviations of $\langle S^2 \rangle$ from zero indicate that the diradical species are not pure singlet spin states. A value of unity for $\langle S^2 \rangle$ indicates a pure diradicaloid state, consisting of an equal mixture of singlet and triplet spin states.³⁵ The anti (**5**) and gauche-out (**7**) transition structures show less mixing with triplet states than intermediate **6**.

We calculated triplet energies for **5**–**7** and used the spin-projection method outlined above to obtain corrected energies which are given in Table 4. These are used with the uncorrected energies to determine energy ranges for structures **5**–**7**.

The spin-correction procedure results in a 1–5 kcal/mol reduction in energy, depending on the degree of triplet mixing in the contaminated singlets, and the differences in energy between the triplet and contaminated singlet states. Transition structures **5** and **7** have less triplet mixing than intermediate **6**. However, the large differences in energy between their contaminated singlet and triplet states result in a greater reduction in energy by the spin-correction procedure.

Activation Entropies. Table 4 lists energies and entropies of stationary points on the Diels–Alder potential surface. The concerted pathway has an activation barrier of 24.8 kcal/mol, while the stepwise process which proceeds through anti transition structure **5** has a barrier in the range of 28.2 to 33.6 kcal/mol. The energy of anti intermediate **6** is between 0.6 and 4.6 kcal/mol less than that of diradical transition structure **5** and 2.8 to 4.2 kcal/mol greater than that of concerted transition structure **3**. While no transition structure for the closure of the biradical intermediate was located, the barrier should be very small.^{1e}

The calculated activation entropy of the concerted pathway is 6 eu more negative than that of the anti stepwise reaction path. At 298 K, the ΔH^\ddagger and ΔG^\ddagger of the concerted pathway are 23.4 and 35.5 kcal/mol, while the corresponding values for the diradical pathway are 27.4 and 37.8 kcal/mol after spin correction. The uncorrected ΔH^\ddagger and ΔG^\ddagger are 32.8 and 43.2 kcal/mol. Thus, the calculated DFT free energy of concert lies in the range of 2.3 to 7.7 kcal/mol. This is in good agreement with Doering’s thermochemical free energy of concert and other

(37) (a) Noodleman, L. *J. Chem. Phys.* **1981**, *74*, 5737. (b) Noodleman, L.; Davidson, E. R. *Chem. Phys.* **1986**, *109*, 131.

(38) (a) Yamaguchi, K.; Jensen, F.; Dorigo, A.; Houk, K. N. *Chem. Phys. Lett.* **1988**, *149*, 537. (b) Yamanaka, S.; Kawakami, T.; Nagao, H.; Yamaguchi, K. *Chem. Phys. Lett.* **1994**, *231*, 25.

Table 5. Calculated Secondary Kinetic Isotope Effects for the Forward and Reverse Concerted Diels–Alder Reactions and the Anti-diradical Diels–Alder Reaction Pathway^a

Concerted Diels–Alder				
	Becke3LYP		CASSCF	MP2
	298.15 K	373.15 K		
H1 = D (out)	0.97	0.98	0.98	0.99
H2 = D (in)	0.92	0.94	0.96	0.95
H3 = D	1.00	1.00	1.02	0.99
H4 = D (in)-endo	0.94	0.96	0.97	0.96
H5 = D (out)-exo	0.95	0.97	0.99	0.98

Retro-Diels–Alder			
	Becke3LYP	CASSCF	MP2
	473.15 K	473.15 K	473.15 K
D ₂ (H4, H5)	1.07	1.09	1.10
D ₄ (H4, H4, H5, H5)	1.15	1.20	1.21

Diels–Alder Diradical Anti T.S. (5)			
	Becke3LYP		CASSCF
	298.15 K	373.15 K	
H _a = D	1.11	1.08	1.10
H _b = D	1.11	1.08	1.11
H _c = D	0.88	0.92	0.92
H _d = D	0.90	0.93	0.93
H _e = D	0.88	0.91	0.93
H _f = D	0.88	0.92	0.93
H _g = D	1.05	1.03	1.05
H _h = D	0.97	0.98	1.02
H _i = D	1.03	1.02	1.03
H _j = D	1.04	1.03	1.06

^a All methods use the 6-31G* basis set. MP2 isotope effects are calculated with unscaled vibrational frequencies, while CASSCF frequencies are scaled by 0.90. RB and UB frequencies are scaled by 0.963 (Rauhut, G.; Pulay, P. *J. Phys. Chem.* **1995**, *99*, 3093). MP2 and CASSCF isotope effects are from ref 1f.

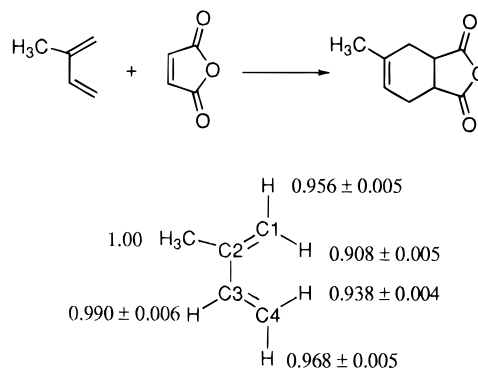
estimates in the range of 2–7 kcal/mol.^{8,39} Relative entropies are also within 3 eu of the CASSCF results.^{1e}

Morokuma and co-workers⁴⁰ have suggested that the computed enthalpy and entropy differences between the concerted boat and chair transition states of the Cope rearrangement are smaller than those that have been measured, because the transition states actually occur not at the C_{2v} or C_{2h} geometries which minimize the electronic energies, but at geometries that minimize the free energies.⁴¹ For the same reason, the computed enthalpy and entropy differences between the concerted and diradical transition states of the parent Diels–Alder reaction may be smaller than the measured values.

(39) Benson, S. W. *Thermochemical Kinetics*; Wiley-Interscience: New York, 1976.

(40) Morokuma, K.; Borden, W. T.; Hrovat, D. A. *J. Am. Chem. Soc.* **1988**, *110*, 4474.

(41) Transition states need to be located using variational transition state theory; (a) Truhlar, D. G.; Garrett, B. C. *Acc. Chem. Res.* **1980**, *13*, 440. (b) Hase, W. L. *Acc. Chem. Res.* **1983**, *16*, 258.

**Figure 5.** Secondary deuterium kinetic isotope effects (298 K) for the reaction of isoprene with maleic anhydride.^{18a}

The entropy of anti intermediate **6** is slightly higher than that of anti transition structure **5**, and significantly higher than that of concerted transition structure **3**. At 298 K the spin-projected and uncorrected free energies of this intermediate are 36.7 and 38.1 kcal/mol, respectively. *Gauche-out* diradical transition state **7** is favored entropically by 1 eu over anti diradical transition structure **5**. This reduces the free energy difference between the anti and *gauche-out* pathways to less than 2 kcal/mol.

Secondary Kinetic Isotope Effects. Secondary deuterium kinetic isotope effects (SKIEs) are a common window through which the transition state of a reaction can be viewed by experiment. Since they provide information on the degree of bond formation or breakage in the transition state of a reaction, SKIEs are an excellent means of differentiating between concerted and stepwise mechanisms. Limited experimental precision in early studies prevented unequivocal differentiation of stepwise versus concerted pathways for the Diels–Alder reaction.^{17,18} However, recent experimental advances have eliminated this problem.^{18a} SKIEs calculated with high-level *ab initio* theory (MP2 and CASSCF) are in excellent agreement with those determined experimentally.^{1f,19a} Here, the RB and UB SKIEs for the concerted and stepwise pathways are compared to those from experiment and other theoretical methods.

Table 5 lists the calculated SKIEs for the concerted mechanism. The RB method predicts inverse SKIEs (373 K) ranging from 0.98 to 0.94 for ethylene and the diene termini. These results compare well with MP2 data, but are larger inverse effects than found with CASSCF calculations.^{1f}

The cause of this discrepancy can be traced to the steric environment of the inside (IN) hydrogens.^{1f} In the concerted DFT transition structure, **3**, they are 0.034 Å closer than those in the CASSCF/6-31G* transition structure. The larger steric repulsion experienced by the IN hydrogens in the DFT structure results in increased out-of-plane bending force constants, and consequently, larger inverse SKIEs. Similar steric arguments explain why the IN inverse SKIEs are consistently larger than the OUT SKIEs.

A recent experimental study of the isoprene plus maleic anhydride Diels–Alder reaction performed by Singleton and co-workers^{18a} provides precise SKIE data (298 K) for each of the hydrogens on isoprene. Summarized in Figure 5, these SKIEs reflect the small degree of asynchronicity induced by the methyl substituent and also show the larger inverse SKIEs for IN versus OUT hydrogens, as predicted by theory.

The RB SKIEs (298 K) for the butadiene plus ethylene reaction are in excellent agreement with the experimental results. Both the H1 OUT and H2 IN SKIEs predicted by DFT differ from the isoprene C1 OUT and IN SKIEs by no more than 1.5%. While the RB H1 OUT SKIE is in excellent agreement with

the isoprene C4 OUT SKIE, the H2 IN SKIE is about 2% more inverse than the isoprene C4 IN SKIE.

As reported previously,^{1f} both inverse and normal SKIEs are found for the stepwise mechanism. The UB inverse effects (298 K) of 10% (H_d) and 12% (H_c, H_e, and H_f) imply a late transition state with advanced σ bond formation. Since the out-of-plane C-H bending force constants of radical centers are smaller than those of alkenes,⁴² normal SKIEs for hydrogens H_a, H_b, H_i, and H_j are predicted. Comparison of the H_a SKIE with that of H_j indicates that hydrogens at primary centers have much larger SKIEs than those at allylic centers. This is in accord with experimental studies.⁴²

The SKIEs predicted for the stepwise mechanism by the UB method are inconsistent with Singleton's experimental results. This theoretical model predicts an H_f inverse SKIE of 12%, while experiment gives only 3% and 4% inverse SKIEs for the C4 and C1 OUT hydrogens. In contrast, the RB H1 inverse SKIE for the concerted pathway is 3%. Thus both experiment and theory support the concerted mechanism.

Conclusions

The concerted and diradical mechanisms for the butadiene plus ethylene Diels–Alder reaction have been compared with

(42) See ref 1f and references therein.

restricted and unrestricted Becke3LYP DFT. A spin-correction procedure for spin-contaminated structures overcorrects for triplet contamination, but allows the energies of the diradical species to be determined within a range of several kcal/mol. Becke3LYP energies are in excellent agreement with experimental data on the heat of reaction and predicted barrier height for the concerted pathway. The ΔG^\ddagger of the stepwise path is predicted to be 2.3–7.7 kcal/mol larger than that of the concerted pathway. The Becke3LYP DFT calculations provide a very promising method for the comparison of concerted and diradical mechanisms.

Acknowledgment. We are grateful to the National Science Foundation for financial support of this research. We thank the UCLA Office of Academic Computing for computer time and facilities. E.G. thanks CSUP for the IBM 590 and Alex Myrman for his assistance.

Supporting Information Available: Tables of energies and coordinates of all structures reported (3 pages). Ordering information is given on any current masthead page.

JA9601494